INVESTIGATION OF LONG-RANGE EFFECT IN GLASSES AFTER ION IMPLANTATION

A. Deshkovskaya
Belarusian State University of Economy,
26 Partizanskiy ave., 220070 Minsk, Belarus, aldesch@mail.ru

The effect of long-range action, propagation of structural disturbances to distances which greatly exceed the penetration depth of implanted atoms, was found in silicate glasses subjected to ion bombardment. Conditions of bombardment: ion energy 60-500 keV, fluence 10^{15}-10^{18} cm^{-2}, current density 1-5 μA/cm^2. As bombarding ions were used: Li^+, Na^+, B^+, N^+, P^+, F^+, Ag^+, In^+, As^+, Sb^+. The presence of this effect is confirmed experimentally by a sharp increase of microhardness of the reverse side of the specimen and changes of its wear resistance. The reason of the long-range action effect is strong dynamic compression of the structural net of the surface layers on the reverse side by shock waves that accompany ion-beam treatment.

Introduction

Bombardment of glass surface with a stream of accelerated ions gives rise to a range of physico-chemical processes, each of them particularly and all of them together can cause the change of glass properties.

One of the effects, which is produced by the ion bombardment, is the long-range effect. The radiation damages, produced by the ion bombardment, appear also beyond the implanted layer boundaries, at depths much larger, than the dopants particles range. This effect is experimentally approved by the results of investigation of the characteristics of the back sides (with reference to the irradiated sides) of the studied samples.

The long-range effect was first observed by Guseva [1, 2] for metals, and further by Pavlov [3] and Uspenskaya [4] for semiconductors.

The long-range effect for glass was discovered by the author in 1977 [5, 6] during the investigation of doped glasses by the thermo- and photostimulated exoelectron emission method. According to the experiments the intensity of the emission current signal from the non-doped (back) side of the sample was three times higher than the signal intensity for this side of the sample before doping. The sample thickness was 0.1-1.5 cm and the dopants penetration depth was not more than 1 μm. It was noticed, that after the samples were annealed at the temperature of 500°C the long-range effect became smaller, but didn't cease.

The aim of this work is to prove the long-range effect through the other experimental methods, such as the investigation of the microhardness, wear-resistance and microrelief of the surface at both sides of the samples before and after ion implantation.

Experiment

The subject under investigation were silicate glasses with simple and complex chemical compositions (Table 1). The samples were prepared as the parallel-sided polished plates with the dimensions of 10x10 (mm^2), 20x20 (mm^2) and disks with the diameter of 10 mm and 1-2 mm in thickness.

One of the sides of the sample was subjected to the ion processing in the implantation or mixing mode. The bombarding ions were selected among the single-charged ions, such as Li^+, Na^+, B^+, N^+, P^+, F^+, Ag^+, In^+, As^+, Sb^+. The energy was 60-500 keV,

Table 1. Chemical composition of the studied glasses

Glass type	Composition, % mass.						
	SiO_2	B_2O_3	Al_2O_3	MgO	CaO	K_2O	Na_2O
Quartz	100	–	–	–	–	–	–
Low-alkali	80.5	12.0	2.0	–	0.5	1.0	4.0
High-alkali	71.3	–	–	3.6	7.0	0.4	15.8

fluence 10^{15}-10^{18} cm^{-2}. The current density was not more than 1μA/cm^2.

The concentration profiles for the dopants depth distribution were calculated according to the program as described in [7].

For the purposes of ion-beam modification of glass in the mixing mode the ion bombardment was conducted through metallic films, which were preliminary deposited onto the glasses surface through the thermal or ion-plasma sputtering. The film thickness was selected according to the dopants projective range values to recoil the atom implantation.

The microhardness was measured by the dynamic ultra-microhardness tester «Shimadzu DUH-200». It's functionality allows to investigate the extremely thin surface layers of the materials and to obtain the microhardness depth distribution profiles.

The preliminary calculations of the dopants depth distribution profiles for the glasses showed, that for the selected interval of the bombarding ions energy (60-500 keV) the dopants concentration maximums are located at the depth of 0.1-0.5 μm from the surface. For the microhardness measurement the probed glass layer depth was much larger – 2.5 μm. The depth of the indenter penetration into the glass was measured with the accuracy of 10 nm. For both sides of the samples the experimental curves of «hardness-to- indenter penetration depth» dependency and the «load-to-Vickers indenter penetration depth» diagrams in the «load-to-deload» mode were studied.

The samples surface microrelief was studied using the «Dektak-800» profilometer. The tribological properties (wear-resistance) were studied through the «needle-on-disk » method with the further utilization of the «Dektak-800» profilometer.

Results and discussion

Fig.1 shows the «load-to-deload» diagrams for the Vickers pyramid in quartz glasses before and

after Na^+ и B^+ ions implantation.

For both cases the Vickers pyramid indentation recovery was produced mostly due to the non-elastic recovery contribution than by the elastic recovery. It is clearly seen at the doped sides of the samples. The curves, obtained for the back sides of the samples, also differ from the curves for these sides before doping. The contribution of the elastic recovery of the pyramid indentation in this case is much higher in comparison to the doped side and to the same side before doping (Fig. 1).

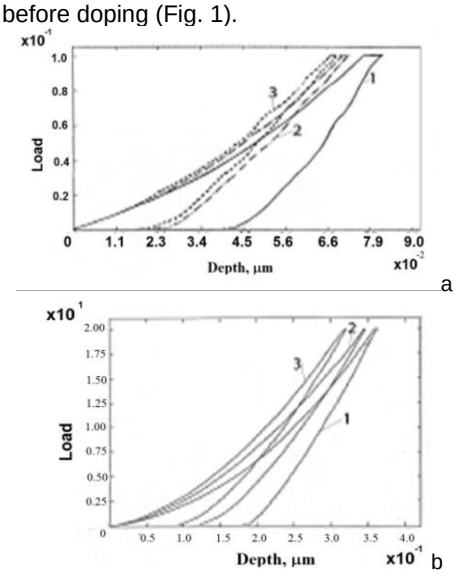

Fig. 1. The «load-to-deload» diagrams for the Vickers pyramid in quartz glasses before and after ions implantation: a - Na^+ (E = 180 keV, F = $6.2 \cdot 10^{16}$ cm^{-2}); b - B^+ (E = 100 keV, F = $3 \cdot 10^{17}$ cm^{-2}). 1 – the doped side; 2 – the original sample (before the implantation); 3 – the back side

Figure 2 gives the examples of the microhardness profiles for the glasses of simple and complex compositions obtained before and after the ion-beam modification.

It is seen from the figures, that the impact of the ion bombardment on the glass microhardness presents not only at the doped side of the samples, but also at the back side, and the level of this effects at the back side is much larger.

For all the studied cases there was the exponential behavior of the microhardness vs depth curves obtained for the back sides of the samples. It was revealed, that after doping the microhardness of the back side was up to 10 times greater than the microhardness of the original surface. The thickness of the layer with a sharp decrease of the microhardness inward the sample is ≈0.7 μm.

The long-range effect is the most significant for the quartz glasses and the less for the multicomponent alkali glass (Figure 2) [8]. It was revealed, that the bombarding ions energy increase as well as the fluence rise result in the long-range effect strengthening. When the samples were annealed the microhadness-depth curves tended to the curves, obtained before the ion-beam processing, but a complete coincidence was not observed. This results show, that the long-range effect suppression produced by the annealing is not entire.

The similar results were obtained for the same

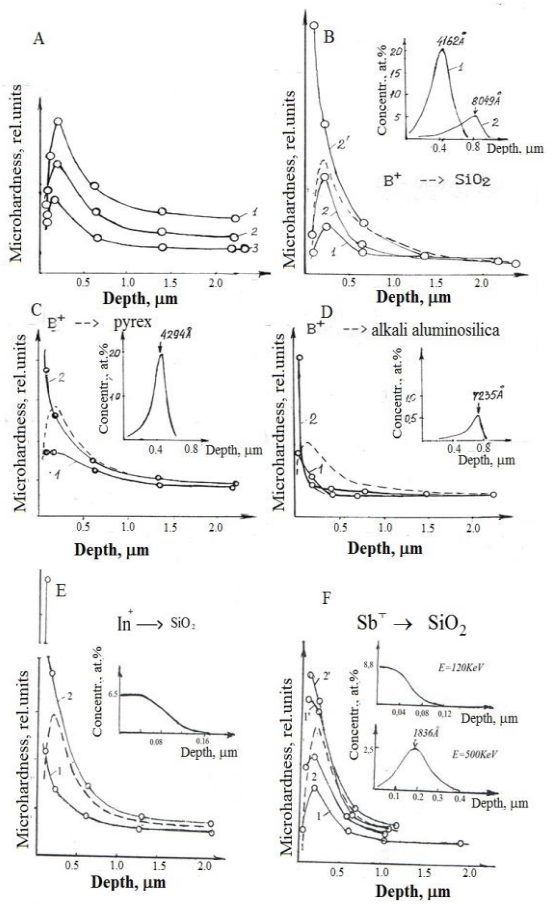

Fig. 2. The microhardness profiles for the silicate glass of various chemical compositions before and after the ion-beam processing: A: 1 – quartz glass, 2 – pyrex, 3 – alkali aluminosilicate glass; B, C, D : B^+ ions doping, dashed line – the original sample (before the implantation);
B: 1 – the doped side (E = 100 keV, F = $3.0 \cdot 10^{17}$ cm^{-2}); 2 – the doped side (E = 200 keV, F = $3.0 \cdot 10^{17}$ cm^{-2}); 2′ – the back side;
C: 1 – the doped side (E = 100 keV, F = $3.0 \cdot 10^{17}$ cm^{-2}); 2′ – the back side; D: 1 – the doped side (E = 100 keV, F = $3.0 \cdot 10^{17}$ cm^{-2}); 2′ – the back side;
E: In^+ ions doping: 1 – the doped side (E = 100 keV, F = $6.0 \cdot 10^{17}$ cm^{-2}); 2′ – the back side;
F: Sb^+ ions doping: 1 – the doped side (E = 120 keV, F = $6.2 \cdot 10^{16}$ cm^{-2}); 1′ – the back side; 2 – the doped side (E = 500 keV, F = $3.0 \cdot 10^{16}$ cm^{-2}); 2′ – the back side

glasses after the ion-beam modification under the mixing mode. The experimental results are given in Fig. 3.

For all the studied cases the roughness of the back side surface was higher than for the original sample before the processing (Table 2) and differed from the doped side.

The surface microrelief investigation at the both sides of the samples before and after the ion-beam processing revealed the difference between the characteristics at various sides and between the unprocessed samples (Table 2). The long-range effect is clearly seen from the swelling presence at the back side of the sample at the 5 and 6 areas boundary, which is the area, located under the doping area 5 of the sample and the area 6 near it, located under the mask. For the quartz glass doped with Ag^+

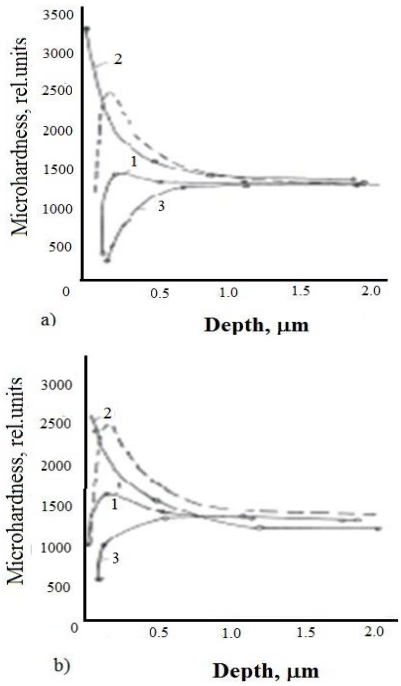

Fig. 3. The ion mixing effect on the glass microhardness profiles: a) 1 – after Ag^+ mixing (Ar^+: E = 200 keV, F = $6.2 \cdot 10^{16}$ cm^{-2}); 2 – the back side; 3 – Ag (600 Å) on the glass before mixing; b) 1 – after Au^+ mixing (Ar^+: E = 200 keV, F = $6.0 \cdot 10^{16}$ cm^{-2}); 2 – the back side; 3 – Au (600 Å) on the glass before mixing. The dashed line describes the original sample

Table 2. The ion-beam modification (IBM) effect on the glass surface microrelief

Glass type	IBM parameters			Roughness, Å			Sample thickness, mm
	Ion	Energy E, keV	Fluence, F, cm^{-2}	Before impl.	Doped side	Back side	
Quartz	B^+	100	$3 \cdot 10^{17}$	13	416	98	1
	P^+	380	$6 \cdot 10^{15}$	13	166	81	1
	Na^+	60	$6 \cdot 10^{17}$	13	24	19	2
	In^+	200	$6 \cdot 10^{17}$	13	15	35	2
Low-alkali	P^+	80	$3.8 \cdot 10^{15}$	13	35	64	2
	As^+	100	$6.2 \cdot 10^{16}$	13	83	53	1
High-alkali	F^+	100	$3 \cdot 10^{17}$	71	185	163	2
		100	$6.2 \cdot 10^{15}$	71	190	93	2
		100	$6.2 \cdot 10^{16}$	35	524	174	2

(E = 200 keV, F = $3.0 \cdot 10^{17}$ cm^{-2}) the swelling was 45-54 Å high. The swelling height for the doping side (4) is much bigger (2955 Å). It should be noted, that the surface roughness of the same sample before the implantation was smaller, than the areas 5 and 6. This effect shows, that the radiation damages particularly penetrate into the area, covered with the mask.

When investigating the character of the Vickers pyramid indentation for various loads, the number of the cracks near the pyramid at the back side of the sample was much smaller, than before the implantation. This is also the result of the long-range effect.

The long-range effect was also registered, when the wear-resistance of the ion-modified glasses was studied. After the abrasive processing of the glasses, subjected and not subjected to the ion bombardment, the groove depth and the amount of the removed material were always different for the doping and back sides of the samples (Fig. 5).

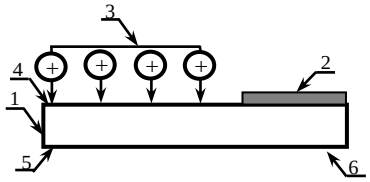

Fig. 4. The image representing the sample and the areas under study: 1 – glass sample, 2 – mask, 3 – bombarding ions flux, 4 – the doping area, 5, 6 – the areas at the back side of the sample: 5 – under the doping area, 6 – under the area covered with the mask

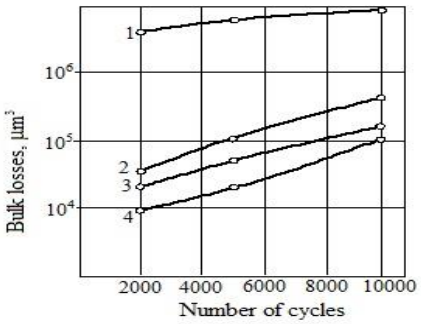

Fig. 5. The wear-resistance of the back side of quartz glasses after the ion implantation: 1 – the original sample, 2 – Na^+ (E = 60 keV, F = $6.0 \cdot 10^{16}$ cm^{-2}), 3 - Na^+ (E = 100 keV, F = $2.5 \cdot 10^{17}$ cm^{-2}), 4 – Ti^+ (E = 100 keV, F = $3.0 \cdot 10^{17}$ cm^{-2})

It should be noted, that the measurement results for all the studied parameters (microhardness, roughness, wear-resistance) were influenced by the time passed between the ion-beam processing and the measurement. The measured parameters changes decreased as the time passed.

This effect reveals the relaxation reorganization of the glass microstructure in all the propagation path of the shock waves, produced by the ion bombardment.

It is impossible to synchronize the conducted measurements in time. The time impact on the measurement results makes the qualitative and quantitative interpretation of the experimental data more difficult.

However, it can be certainly stated, that in the process of dose gaining while the glass ion bombardment, its structural net elements are subjected to the elastic deformation, which penetrates into the sample as the shock wave and if the absorbed energy amount is high enough reaches the back side and reflects from it.

The shock wave propagation, involving the new structural elements into the effect produces the observed long-range effect.

Conclusion

The experimental investigations of the glasses of three types after implantation with various ions (with the following parameters: E = 60 keV, F = $6.0 \cdot 10^{16}$ cm^{-2}) proved the presence of the long-range effect. The effect is characterized by penetration of the radiation damages, produced by the ion bombardment, inward the sample, and the consequent changing of the properties of the back side,

such as the microhardness, wear-resistance, crack-resistance and surface microrelief.

The observed effect is produced by the following: in the dose gaining process there are alternating stresses occurring in the glass. These stresses penetrate inward the sample along the ion beam direction in the form of shock waves, which reach the back side of the sample, reflect from it many times, thus leading to the accumulation of the structural damages in glass and producing the local tightening in it. The long-range effect intensity decreases with time. It is caused by a slow relaxation of the structural damages, which were produced by the ion bombardment.

Acknowledgements: In conclusion the author express her gratitude to the authorities of the Institute of ion-beam physics and materials research in Rossendorf (Germany) (Dr.nat. Richter E., Prof. Möller W.) for the provided opportunity of experimental research.

References

1. *Guseva M.I., Aleksandriya B.V.* // JAP. 1961. V. 31. № 6. P. 867-875.
2. *Guseva M.I.* // Surface. Physics, Chemistry, Mechanics. 1982. № 4, Pp. 27-50.
3. Pavlov P.V., Popov Yu.S., Belich T.V. // Physics and techniques of semiconductors. 1974. V.8. № 5. P. 936.
4. *Uspenskaya G.I*. Synopsis of a Ph.D. thesis. Gorkiy, 1976. 18 p.
5. Deshkovskaya A. Mat. of the 2 All. Union Symp. «Exo-electron Emission and its. Application». Moscow, May, 1982. P. 36-37.
6. *Deshkovskaya A., Zatsepin A.F., Tyukov V.V.* Mat. of the IV All. Union Symp. «Exoelectron Emission and its. Application». Tbilisi. 1985. P. 67-68.
7. *Zeigler J.F., Biersack J.F., Littmark K.* The stopping and Range of Ions in Solids. Pergamon, New York. 1985.
8. *Deshkovskaya A.* Proceedings of the 9th International Conference IRS-2011. Minsk, Belarus. September 20-22. 2011. P. 213-215.

STRUCTURE CHANGES IN SILICON IRRADIATED BY HIGH ENERGY IONS OF HYDROGEN, DEUTERIUM AND HELIUM

Margaryta Starchyk[1)], Galyna Gaidar[1)], Larysa Marchenko[1)], Myroslava Pinkovska[1)], Volodymyr Popov[2)], Galyna Shmatko[1)], Valentina Varnina[1)]

[1)]*Institute for Nuclear Research of NAS of Ukraine, 47 Nauky ave., 03680 Kyiv, Ukraine, myrglory@yahoo.com*

[2)]*"RIM" STC "Institute for Single Crystals" of NAS of Ukraine, 3 Severno-Syretskay str., 04136 Kyiv, Ukraine, info@imd.org.ua*

Structural and optical properties of silicon irradiated by ions of 6.8 MeV hydrogen (p^+ or H^+), 13.6 MeV deuterium (heavy hydrogen $^2H^+$ or D^+) and 27.2 MeV helium (α-particles or He^{2+}) with fluences $\Phi \geq 5 \cdot 10^{16}$ cm^{-2} were studied using the complex of methods: selective etching and metallographic, ellipsometry and profilometry. The irradiated crystals were cut along the direction of irradiation, allowing to study the properties of silicon in the region of the ions' path, braking and behind it. The projection lengths of the path of the ions of a given energy are about 360 microns for p^+ and He^{2+} and about 780 μm for D^+.

The main structural defects are observed in the braking region, where concentration of radiation defects is the largest. The widths of etched lines along ion stopping change in the direction from the sample edge (where temperature was lower due to the sample cooling during irradiation) to the center of irradiation and depend of the ion type.

After proton irradiation silicon structure in the path region does not sufficiently change. Structure of the path region of helium irradiated Si changes essentially from the crystal form to the highly destroyed (perhaps, polycrystalline). At currents about 0.25 - 0.45 μA and fluences $\Phi \geq 10^{16}$ cm^{-2} the defect "walls" parallel to the stopping line appeared both in the path region, and behind stopping line at the distance equal to double projection length of the path. The number of the "walls" depended on the ion beam intensity.

We consider that the soliton mechanism is responsible for the ordered structure creation in the region behind the stopping line. Periodic structures in the path region might appear due to the moving of the recrystallization front of the highly disordered layers, possible, amorphous, in the process of the highly energetic long-lasting ion irradiation.

Introduction

Modern radiation doping of semiconductors by ion beams is characterized by the creation of layers with different from matrix properties due to controlled input of impurities and defects. The method makes it possible receiving of hidden layers with other conductivity type, forming of p-n-junctions, passivation of tensions and defects and getting of new electrical and photovoltaic characteristics.

Currently the behavior of nonequilibrum system of defects under long-lasting energetic irradiation has not been established jet and the influence of ions with about tens MeV energy range on silicon properties is the least studied. We present the data of structural changes of Si, irradiated by 6.8 MeV hydrogen (protons), 13.6 MeV deuterium (deuterons), and 27.2 MeV helium (α-particles) ions with fluences $\geq 5 \cdot 10^{16}$ см$^{-2}$ and show the perspective to use such ion beams for radiation doping technology.

Experiment

Structural and optical properties of ion irradiated silicon crystals were studied by the complex of methods: selective etching and metallographic, ellipsometry and profilometry. Silicon crystals, grown by the Czochralski and floating-zone methods, with dislocations ($N_D \approx 10^4$ cm^{-2}) and without them were used. Samples were grinded, polished, etched and irradiated by light ions (6.8 MeV protons, 13.6 MeV deuterons, and 27.2 MeV α-particles) by fluences $\geq 5 \cdot 10^{16}$ cm^{-2} in cyclotron U-120 of Institute for Nuclear Research of NAS of Ukraine. The irradiation temperature was ≤ 100 °C, as during irradiation the